LIMNOLOGY and OCEANOGRAPHY

ASLO

Limnol. Oceanogr. 67, 2022, 934–945

doi: 10.1002/lno.12046

Measurement of microplastic settling velocities and implications for residence times in thermally stratified lakes

Hassan Elagami,[1,2*] **Pouyan Ahmadi**,[3] **Jan H. Fleckenstein**,[3,4] **Sven Frei**,[2] **Martin Obst**,[5] **Seema Agarwal**,[6] **Benjamin S. Gilfedder**[1,2]

[1]Limnological Research Station, Bayreuth Center of Ecology and Environmental Research, University of Bayreuth, Bayreuth, Germany
[2]Department of Hydrology, Bayreuth Center of Ecology and Environmental Research (BayCEER), University of Bayreuth, Bayreuth, Germany
[3]Department of Hydrogeology, Helmholtz Centre for Environmental Research – UFZ, Leipzig, Germany
[4]Hydrologic Modelling Unit, Bayreuth Center of Ecology and Environmental Research (BayCEER), University of Bayreuth, Bayreuth, Germany
[5]Experimental Biogeochemistry, BayCEER, University of Bayreuth, Bayreuth, Germany
[6]Macromolecular Chemistry II, University of Bayreuth, Bayreuth, Germany

Abstract

Microplastics residence times in lakes are currently poorly understood. In this work, settling experiments with pristine and biofilm-colonized microplastic particles were combined with model calculations to evaluate settling velocities, particle distributions, and residence times in the epilimnion, metalimnion, and hypolimnion of a hypothetical stratified lake broadly based on Upper Lake Constance. Settling velocities of various biodegradable and nonbiodegradable polymers of various shapes, sizes, and biofilm colonization were measured in a settling column. The settling velocities ranged between ~ 0.30 and ~ 50 mm s^{-1}. Particle sizes and polymer densities were identified as primary controls on settling rates. Microplastic particles that had been exposed to a lake environment for up to 30 weeks were colonized by a range of biofilms and associated extracellular polymeric substances; surprisingly, however, the settling velocity did not vary significantly between pristine and colonized microplastic particles. Simulated microplastic residence times in the model lake varied over a wide range of time scales (10^{-1} to 10^{5} d) and depended mainly on the size of the particles and depth of the lake layer. Long residence times on the order of 10^{5} d (for 1-μm microplastic particles) imply that for small microplastic particles there is a high probability that they will be taken up at some stage by lake organisms. As the lake retention time (~ 4.5 years) is considerably shorter than the residence time of small microplastics, negligible quantities of these microplastic particles should be found in the lake sediment unless some other process increases their settling velocity.

*Correspondence: hassan.elagami@uni-bayreuth.de

Additional Supporting Information may be found in the online version of this article.

Author Contribution Statement: H.E. performed the laboratory experiments, whole lake modeling and worked on the manuscript. P.A. and J.H.F. assisted in data interpretation and writing the manuscript. S.F. developed the whole lake model, conducted the simulations, and contributed to writing the manuscript. M.O. performed the confocal laser scanning microscopy and assisted with analysis and interpretation of the biofilm data. S.A. provided the microplastics, and assisted in data interpretation from the settling column, especially relating to the surface chemistry of plastic polymers. B.S.G. conceived the project, and assisted in data interpretation and writing and editing the manuscript.

Over the past 70 years, plastic polymers have established themselves as cost-effective and durable materials that are used ubiquitously in industry, agriculture, and domestic applications. In 2015, global annual production of plastic polymers reached ~ 322 Mt (Worm et al. 2017). Roughly 50% of the plastic volume produced is made for single-use applications, and in particular for packaging purposes (Worm et al. 2017). By 2015, ~ 6300 Mt of plastic waste had been produced, of which approximately 9% was recycled, while 79% accumulated in landfills and the environment (Geyer et al. 2017). The majority of the plastic debris found in nature are high molar mass polymers such as polyethylene and polyethylene terephthalate (Agarwal 2020).

Rivers and streams are considered the dominant transport pathway moving plastic from terrestrial sources to the marine

sink (Fischer et al. 2016). In contrast to fluvial systems, lakes and reservoirs are mostly considered as permanent or temporary sinks for plastics due to their low-energy hydrodynamic regimes. Plastics in lakes and rivers originate predominantly from terrestrial sources such as effluents from waste-water treatment plants (Sun et al. 2019), agriculture, and improper dumping of plastic waste (Bellasi et al. 2020). During the transport of plastic in freshwater systems, it is exposed to various physical, chemical, and biological degradation processes (Browne et al. 2007; Meides et al. 2021). Fragmentation and degradation processes in natural environments transform plastic fragments larger than 5 mm into microplastics < 5 mm (Arthur et al. 2009) and nanoplastics (Toussaint et al. 2019).

As the density of pristine nonbuoyant plastic polymers lies close to that of water, microplastics are expected to remain in suspension for a substantial time before sedimentation to lake sediments. Long residence times in the water column increases the probability of uptake by organisms such as zooplankton (Nguyen et al. 2020) as such organisms cannot differentiate between microplastics and natural particulate matter used as food (Aljaibachi and Callaghan 2018).

Once microplastics have entered the food chain, organisms including zooplankton and fish uptake microplastics through ingestion via predation (Nelms et al. 2018). After microplastics have been ingested, they can also be egested within fecal pellets (Cole et al. 2016). As fecal pellets are a source of food for many aquatic organisms, the ingestion of these microplastic-containing pellets facilitates the transfer of microplastics to various trophic levels (Nelms et al. 2018). Fecal pellets may also form a pathway for microplastic sedimentation, removing them from the lake water column (Cole et al. 2016), although this remains poorly understood.

Existing studies have proposed that the physical properties of microplastics such as polymer density, shape, and size control the settling velocity of pristine microplastics (Khatmullina and Isachenko 2017; Waldschläger and Schüttrumpf 2019) and the residence time in the water column (Nguyen et al. 2020). Since most of microplastics in aquatic systems are irregularly shaped, they tend to have a larger surface area compared to spherical particles. The high surface area of the irregular particles leads to increased hydrodynamical friction and drag forces, resulting in lower settling velocities compared to ideal spheres (Dietrich 1982).

Pristine microplastics are also exposed to various types of biofilm-building microorganisms over time scales that are largely dependent on residence times of the particles in the water column and polymer properties (Zettler et al. 2013; Leiser et al. 2020; Ramsperger et al. 2020). Also, the hydrophobic nature of pristine microplastics favors biofilm formation (Zettler et al. 2013; Rummel et al. 2017; Lacerda et al. 2019). Accumulation of biofilms and attachment of microorganisms on the surfaces of pristine microplastics can potentially alter their density (Rummel et al. 2017; Michels et al. 2018) and thus their settling velocities (Kaiser et al. 2017). While some studies have suggested that the development of biofilms on microplastic surfaces increases the settling velocity (Kaiser et al. 2017), other recent studies have found no substantial changes in the settling rates (Leiser et al. 2020). However, there is still very little known about how the physical, biological, and chemical conditions in lakes (which are very different from oceans) affect the formation of biofilm on microplastics and how this affects their settling behavior (Leiser et al. 2020). For example, biofilms may make the surface of colonized particles "stickier," facilitating the formation of aggregates with other suspended materials such as mineral sediments or organic matter (Rummel et al. 2017).

The temperature gradient in the stratified lake water column is associated with changes in the density and the viscosity of water. As a consequence, drag forces exerted on particles increase from the relatively warm epilimnion (lower viscosity) to the cold hypolimnion (higher viscosity). Microplastic transport is also influenced by turbulence occurring in the epilimnion, which is mainly driven by wind (Singh et al. 2019), and in the hypolimnion caused by internal hydrodynamic forces such as seiches, currents, and bed roughness (Kirillin et al. 2012; Nishri et al. 2015). Compared to laminar conditions in the metalimnion, turbulent mixing in the epilimnion and hypolimnion likely causes resuspension of the settling particles and increases their residence time in these zones (Reynolds 2006, pp. 70–71). Due to the largely laminar conditions in the metalimnion, the residence time of microplastics only depends on the settling velocity of the particle and the thickness of the layer.

In this work, we combine systematic laboratory experiments, lake incubations, and model calculations to understand the effect of microplastic properties on sedimentation behavior. We then estimate the residence time, accumulation in, and transfer of microplastics between, lake compartments via virtual lake simulations. The residence time is presented as a critical parameter for determining accumulation of microplastics in the water column and potential uptake and transfer within the lake ecosystem. We anticipate that the residence times of pristine microplastics are controlled by the physical properties of the particles, as well as lake properties, such as turbulent mixing and depth.

Methods

Characterization of microplastic particles

All biodegradable and nonbiodegradable fragments were provided by the Department of Macromolecular Chemistry at the University of Bayreuth, Germany. The selected polymers (Table 1) capture the dominant plastics produced by the plastic industry (Wright et al. 2013; Rocha-Santos and Duarte 2015). The size of the particles ranged between ~ 150 and ~ 2200 μm. The selection of various particles and polymer types aimed at assessing the effect of particle size, and polymer density on the settling velocity. The distinction between

Table 1. A list of all polymers used during settling velocity experiments and their measured densities.

Polymer	Abbreviation	Density (g cm^{-3})	Type
Polystyrene	PS	1.03	Nonbiodegradable
Polyamide 66	PA66	1.12	Nonbiodegradable
Polyvinylchloride	PVC	1.38	Nonbiodegradable
Polycaprolactone	PCL	1.14	Biodegradable
Polylactide	PLLA	1.20	Biodegradable
Polybutylenadipate terephthalate	PBAT	1.22	Biodegradable

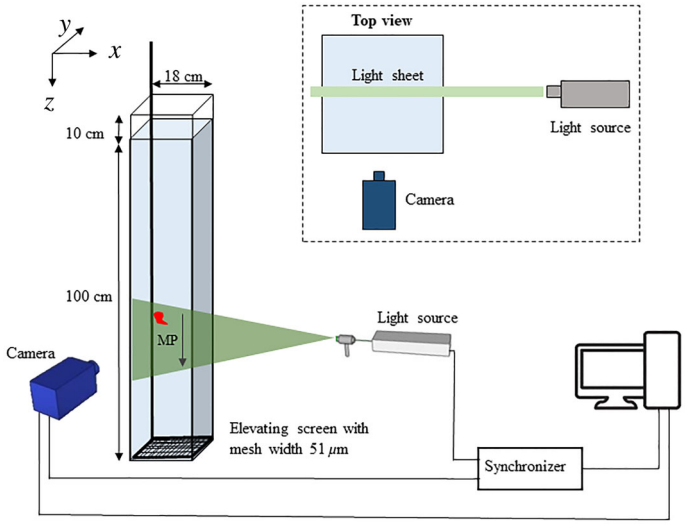

Fig. 1. The water column and the setup of the two-dimensional particle image velocimetry system.

biodegradable and nonbiodegradable polymers was aimed at assessing the potential effect of polymer surface chemistry and polymer type on the settling behavior of microplastic particles in lakes. Also, several recent studies, such as Bagaev et al. (2017) and Waldschläger and Schüttrumpf (2019), focus mainly on non-biodegradable polymers. Our work extends the types of polymers assessed in sinking experiments to a potentially important class of plastics that may become more prevalent in the future as society move toward biodegradable plastics.

Particle geometries were determined in the laboratory using a light microscope and a high definition digital single-lens reflex camera (Zeiss Axioplan microscope and Cannon EOS 5D respectively). The maximum particle length A [L] and the minimum particle length C [L] in the XY-plane of each irregularly shaped particle were measured based on these images using ImageJ software (Schindelin et al. 2012) (Supporting Information Fig. S1). The XZ-plane length B [L] was estimated as the average of A and C as a necessary approximation due to only being able to acquire two-dimensional images with the microscope available. As all particles used in the experiments were irregularly shaped (Supporting Information Fig. S1, S2), the equivalent diameter of each particle was calculated based on the best-fitting ellipsoid. The equivalent spherical diameter for each particle D_{eq} [L] was then calculated according to Eq. 1 using the value from the ellipsoid. The Corey shape factor (CSF) was also calculated as in Eq. 2. The CSF is widely used to describe the overall shape of the particles and can be calculated as the thickness of the particle divided by the geometric average of the other two dimensions. It ranges from 0 to 1.0 and it is correlated with particle flatness.

$$D_{eq} = \sqrt[3]{ABC}, \quad (1)$$

$$\mathrm{CSF} = \frac{C}{\sqrt{A.B}}. \quad (2)$$

The density of each nonbuoyant polymer was determined according to the procedure described in Waldschläger and Schüttrumpf (2019): Each particle was placed in a 50-mL glass beaker of distilled water. After the particle had sunk to the bottom, 1 μL of zinc chloride solution was added. This procedure was repeated until the particle was in a stable suspension. One milliliter of the solution was then weighed to determine the density of the particle. This process was repeated three times for each polymer using three different particles and the average polymer density was calculated. Some of the particles initially did not sink, despite their densities exceeding that of water. This is thought to be due to the hydrophobic surface chemistry of the pristine plastic. To avoid this, the particles were pretreated for 20 min in an ultrasonic bath. The hydrophobicity effect was particularly noticeable for polystyrene as its polymer density 1.03 g cm^{-3} is very close to that of water.

Settling velocity measurements

Settling velocities of the microplastic particles were measured in a water-filled glass column with a cross-section of 18 cm × 18 cm and a height of 1.10 m (Fig. 1) based on the design of Khatmullina and Isachenko (2017). At the bottom of the column, a filter mesh (width 51 μm) was used to collect and retrieve the individual particles after each settling experiment. The glass column was also equipped with two thermometers to measure the water temperature during each experiment. The laboratory was air-conditioned at 20 ± 1°C. Settling velocities were measured using tap water (density = 0.998 g cm^{-3}, kinematic viscosity = 0.01 cm^2 s^{-1}, and oxygen content = 9.45 mg L^{-1}).

The settling velocity for each microplastic particle was determined using a two-dimensional particle image velocimetry system iLa 5150. The system consists of a high-speed camera (80 frames per second), a light source (high-power light-emitting diodes) with a wavelength = 530 nm, and hardware for synchronization (Fig. 1). The software can determine the settling velocities in two dimensions using the recorded image stream by cross-correlation of sequential pairs of images. The image pairs were used to analyze the settling path of each particle and the time elapsed. The system was tested for accuracy and precision. A reference particle (polyamide 66) with an equivalent diameter of 1.75 mm was measured seven times under identical conditions. After each measurement, the particle was collected using the mesh. The mean and relative standard deviation (RSD%) was 32 mm $s^{-1} \pm 7\%$.

Each particle was lowered slowly into the settling column using tweezers and released a few centimeters below the water surface. The settling velocity of each particle was measured after the particle had reached its estimated (Stokes) terminal velocity and a stable orientation in the water column. The particle image velocimetry setup was placed at the lowest third of the settling column. In total, between 60 and 70 settling experiments were conducted for each polymer amounting to a total of about 400 settling experiments.

Lake incubations

To measure the effects of biofilm colonization on microplastic settling behavior, polyamide 66, polystyrene, polyvinylchloride, polycaprolactone, polylactide, and polybutylenadipate terephthalate particles with a size range from 300 to 2200 μm, used previously as part of the settling experiments, were incubated in a pond close to the University of Bayreuth. All incubations started in January and the incubation periods were 6, 8, 10, and 30 weeks. Each particle was incubated in a separate glass tube that was sealed at both ends using stainless steel screens with a mesh size of 51 μm (Supporting Information Fig. S3). This design allowed microorganisms to enter the tubes and to colonize microplastic particles but did not allow the particles to be lost from the tubes. Several polystyrene particles (300 to 350 μm) were incubated in the same tube for 10 weeks to investigate potential particle–particle interactions and how this may be influenced by biofilms. The changes in size, density, and shape of each incubated particle were characterized following the same procedures as described for the pristine particles.

Colonization of microplastic particle surface with biofilm-building microorganisms was characterized by confocal laser scanning microscopy. Colonized microplastic particles were incubated in 100 μL staining solution for 20 min. All dyes and lectin-dye conjugates were used in a concentration of 1 μg ml^{-1}. DNA/RNA was stained using Syto 40. The DNA/RNA signal was used to visualize microbial cells whereas lectin-fluorophore conjugates were used to visualize the extracellular polymeric substances (wheat germ agglutinin—Alexa Fluor 555, soybean agglutinin—Alexa Fluor 488, and peanut agglutinin—Alexa Fluor 647). After incubating the particles in the dyes, the samples were rinsed three times with tap water. Aggregates were analyzed in a Petri dish in their original hydrated condition. The images were collected with $\times 10$ and $\times 20$ water immersion lenses with numerical apertures of 0.3 and 0.6, respectively.

Finally, after incubation, the changes in the settling velocity of each particle were evaluated by comparing the settling velocity between the pristine and incubated particles. The density of the incubated particle was determined after the settling velocity measurements to keep the biofilm in its original state as the zinc chloride solution is likely to destroy the biofilm structure. In addition, the settling column was filled with filtered lake water so that changes in osmotic pressure would not disturb the delicate biofilm structure. The density and the viscosity of the filtered lake water were determined in the laboratory. The physical properties of the filtered lake water were essentially the same as tap water.

Settling velocity model

As most of the particles were irregularly shaped and relatively large (> 0.1 mm) (Supporting Information Figs. S1, S2), the hydrodynamic flow conditions around the particles were likely to be at Reynolds number > 1.0. To account for the nonspherical geometry of the particles the semiempirical model of Dietrich (1982) was used to calculate the theoretical settling velocities. Rather than expressing the results in the terms of Reynolds number and drag coefficient, Dietrich (1982) uses the terms of dimensionless particle size and dimensionless settling velocity (Supporting Information Eq. S4a–f). For small particles, Dietrich (1982) converges on Stokes' law (at about a dimensionless particle size less than 2.0). For the "large" particles, the model accounts for the progressive growth in the flow field separation which increases the drag pressure more rapidly for a given increase in the settling velocity. However, Dietrich (1982) notes that the equation should not be used for dimensionless particle size greater than 5×10^9 as the boundary layer around the particles becomes fully turbulent, reducing the flow separation and thus pressure drag. The Reynolds number and dimensionless particle size were checked for each particle to investigate the flow regime around the particles. The settling velocity formulas are presented in the Supporting information (Eq. S4a–f).

Continuum model for microplastic particles in a stratified lake

The residence times and particle number within a hypothetical lake system and the flux between lake compartments (epilimnion, metalimnion, and hypolimnion) were modeled using a generic continuum model for vertical microplastic transport. The model represents a lumped parameter approach

consisting of three interacting model sub-systems representing the epilimnion, metalimnion, and hypolimnion. For the epilimnion and hypolimnion, the model assumes fully mixed (turbulent) conditions represented by exponential transfer functions (i.e., exponential residence time distributions) as first implemented by Reynolds and Wiseman (1982) and Reynolds (1984, pp. 46–50) and summarized by Reynolds (2006, pp. 70–71) and Lampert and Sommer (2010, pp. 48–49). In this approach, rather than representing the hydrodynamic conditions of the different lake compartments explicitly using, for example, an eddy diffusion coefficient and calculating fluxes in one dimension, the effect of turbulent mixing was simplified using the transfer functions so that each sub-system could be treated as zero-dimensional. In reality, this means that the eddy diffusion coefficient is large enough that the system can be treated as well mixed on timescales relevant for microplastic transport. For the metalimnion, the model assumes laminar flow conditions and settling behavior, where particles have a single residence time. The combination of the three lake compartments gives a set of three differential equations that are solved simultaneously (Eq. 3a–c):

$$\frac{dN_{\mathrm{epi}}}{dt} = \dot{N}_{\mathrm{in}} - k_{\mathrm{epi}} N_{\mathrm{epi}}(t), \tag{3a}$$

$$\frac{dN_{\mathrm{meta}}}{dt} = k_{\mathrm{epi}} N_{\mathrm{epi}}(t) - k_{\mathrm{epi}} N_{\mathrm{epi}}(t - \tau_{\mathrm{meta}}), \tag{3b}$$

$$\frac{dN_{\mathrm{hypo}}}{dt} = k_{\mathrm{epi}} N_{\mathrm{epi}}(t - \tau_{\mathrm{meta}}) - k_{\mathrm{hypo}} N_{\mathrm{hypo}}(t). \tag{3c}$$

Equation 3a describes the dynamic change of microplastics in the epilimnion, where $\dot{N}_{\mathrm{in}}$ [particles T^{-1}] represents a defined input flux of particles into the lake (e.g., via an inflowing river), $-k_{\mathrm{epi}} N_{\mathrm{epi}}(t)$ [particles T^{-1}] is the loss of particles to the metalimnion, and k_{epi} [T^{-1}] is a first-order exchange coefficient. Equation 3b calculates the microplastic particles in the metalimnion where τ_{meta} [T] is the residence time of the particles. The particle flux from the metalimnion into the hypolimnion is $-k_{\mathrm{epi}} N_{\mathrm{epi}}(t - \tau_{\mathrm{meta}})$ [particles T^{-1}] while Eq. 3c represents the dynamic change of particles in the hypolimnion. The loss of particles from the lake to the sediments is $k_{\mathrm{hypo}} N_{\mathrm{hypo}}(t)$ [particles T^{-1}] where k_{hypo} [T^{-1}] is a first-order exchange coefficient similar to that in the epilimnion. The first-order exchange coefficients k_{epi} and k_{hypo} [T^{-1}] were calculated by $k_{\mathrm{epi,hypo}} = \frac{1}{\tau_{\mathrm{epi,hypo}}}$ with τ [T] being the mean residence time in each respective layer.

In the well-mixed layers, the residence times τ_{epi} [T] and τ_{hypo} [T] were defined as the time required until the particle number was reduced to $1/e \approx 0.368$ (i.e., 36%) of the initial

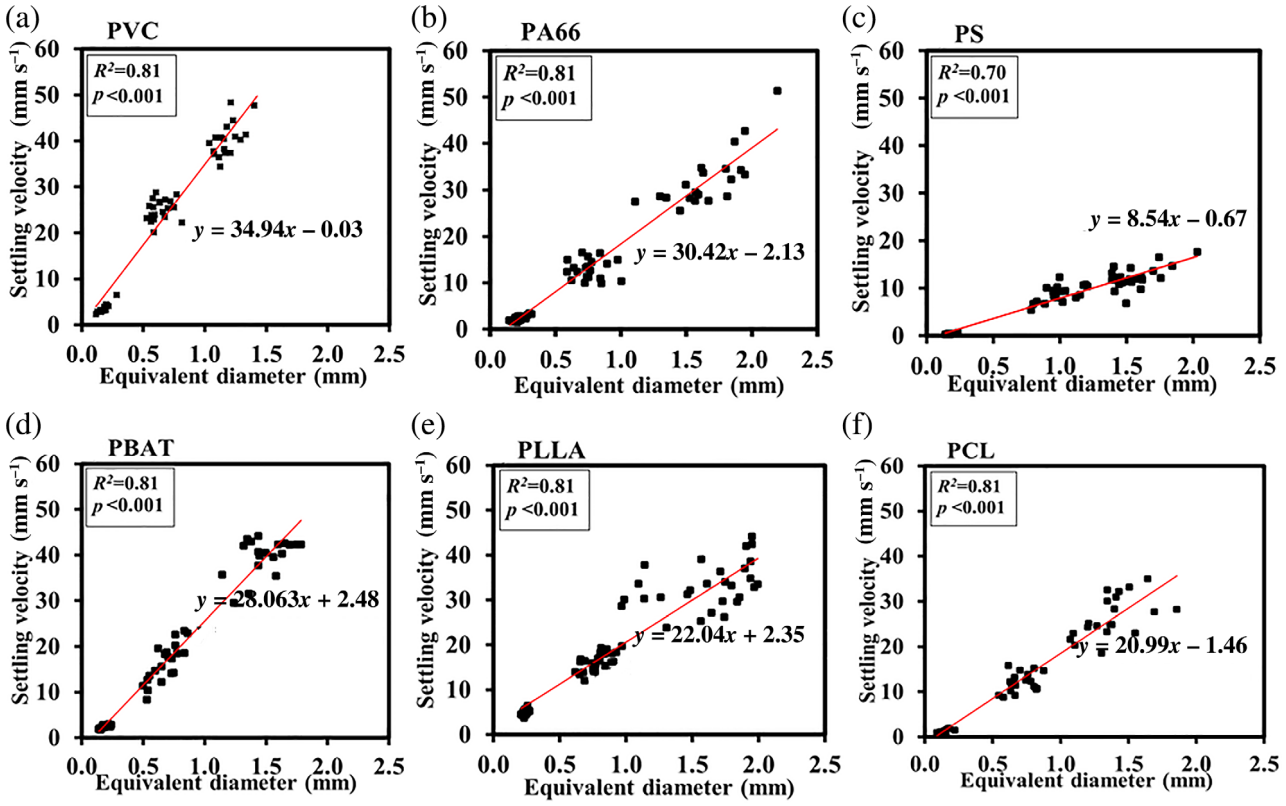

Fig. 2. Results of the experimentally measured settling velocities vs. equivalent diameter of the polyvinylchloride (PVC), polyamide 66 (PA66), polystyrene (PS), polybutylenadipate terephthalate (PBAT), polylactide (PLLA), and polycaprolactone (PCL) fragments, where p is the probability obtained from the t-test, R^2 (–) is the coefficient of determination, and the red line represents the regression line.

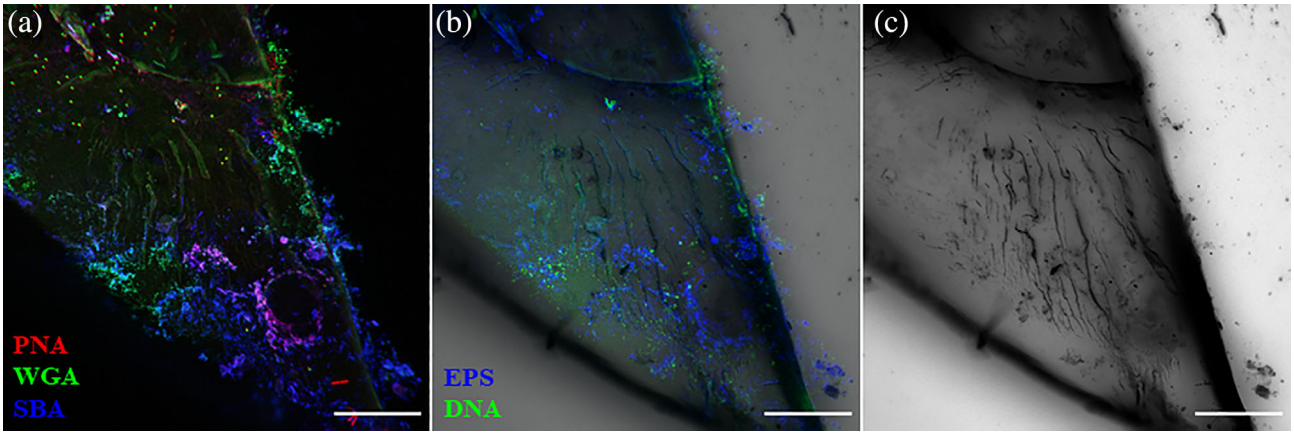

Fig. 3. Confocal laser scanning microscope images for the extracellular polymeric substances (EPS matrix) and microbial cells (DNA) colonizing the surfaces of a polyamide 66 particle after 10 weeks of incubation. (**a**) Peanut agglutinin (PNA), wheat germ agglutinin (WGA), and soybean agglutinin (SBA) lectins visualize the EPS matrix in a red, green, and blue overlay; (**b**) the EPS matrix and DNA are visible on the particle; and (**c**) the surface of the microplastic is shown in gray scale. The length of the scale bar is 150 μm.

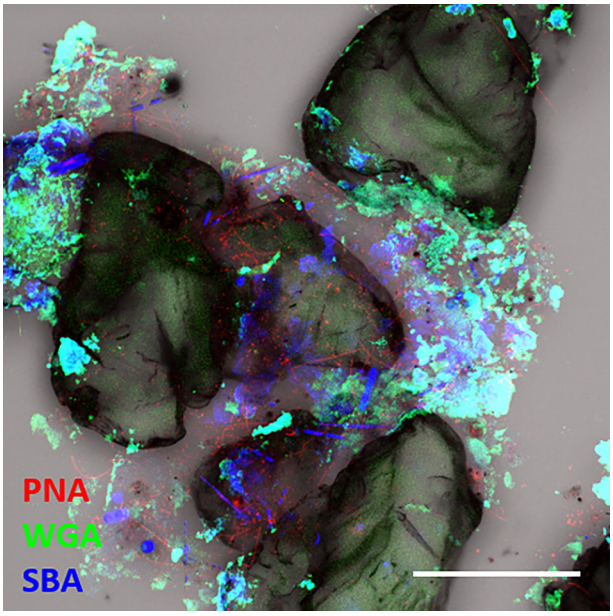

Fig. 4. A confocal laser scanning microscope image of the aggregation of polystyrene particles after 10 weeks of incubation. Peanut agglutinin (PNA), wheat germ agglutinin (WGA), and soybean agglutinin (SBA) lectins visualize the EPS matrix in a red, green, and blue overlay. The length of the scale bar is 150 μm.

particle concentrations (Reynolds 2006, pp. 70–71). The residence time in the metalimnion τ_{meta} [T] was calculated by dividing the thickness z_{meta} [L] of the layer by the laminar settling velocity of the particle. Values for the mean residence time were estimated according to Eq. 4, where v_s [LT^{-1}] represents the laminar settling velocities for microplastics in the relevant lake compartment and z [L] is the corresponding thickness of the epilimnion, metalimnion, or hypolimnion.

$$\tau_{epi,meta,hypo} = \frac{z_{epi,meta,hypo}}{v_{s\_epi,meta,hypo}}. \quad (4)$$

For simplicity, and to illustrate the effect of microplastic particle size on residence time, the model was run using settling velocity data from polystyrene spheres. The laminar settling velocities of the polystyrene spheres (1, 10, 500, and 1000 μm) were measured using the same procedures mentioned before. To account for the changes in the settling velocities of the microplastics due to the change of the water temperature in each lake compartment, the settling velocities were corrected as in Ghawi and Kris (2012) using their eq. S5. The dynamic model was constructed and solved using the Simulink toolbox included in MATLAB.

In addition to the dynamic model above, a simplified steady-state solution for Eqs. 3a–c assuming a constant particle influx $\dot{N}_{in} = \text{const}$, was derived for the particle number in each lake compartment:

$$N_{epi} = \frac{\dot{N}_{in}}{k_{epi}} = \dot{N}_{in}\tau_{epi,} \quad (5a)$$

$$N_{meta} = \frac{\dot{N}_{in}}{k_{epi}}\left[e^{(k_{epi}\tau_{meta})} - 1\right], \quad (5b)$$

$$N_{hypo} = \frac{\dot{N}_{in}}{k_{hypo}} = \dot{N}_{in}\tau_{hypo}. \quad (5c)$$

This steady-state solution was used to quantify the relative distribution of microplastic particles in each lake compartment of thermally stratified lakes. In particular, the ratio between particles located in the epilimnion and hypolimnion (N_{epi}/N_{hypo}) was used as a characteristic parameter to compare lake systems. This ratio can be used to rapidly determine if most microplastic particles will be found in the epilimnion or the hypolimnion, which is important as the epilimnion is where microplastics are most likely to be taken up by organisms such as filter feeders. In this model, the ratio N_{epi}/N_{hypo} only

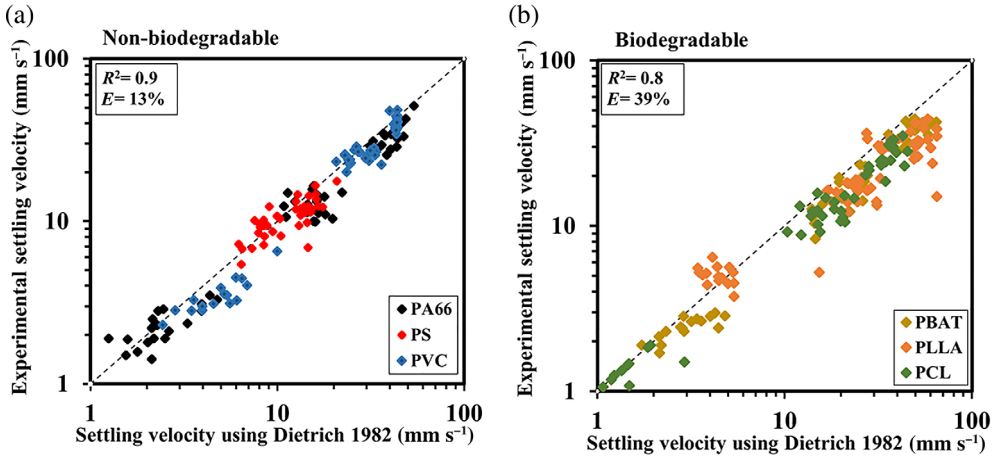

Fig. 5. A comparison between the experimental settling velocities and Dietrich model for the nonbiodegradable polyvinylchloride (PVC), polyamide 66 (PA66), polystyrene (PS), and biodegradable polybutylenadipate terephthalate (PBAT), polylactide (PLLA), and polycaprolactone (PCL) particles, where E is the relative error (%), and R^2 (−) is the coefficient of determination. The dashed line presents the 1 : 1 line.

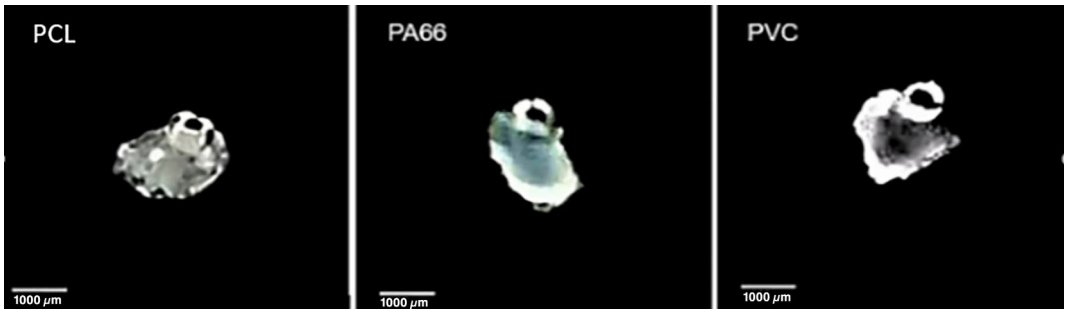

Fig. 6. Attachment of fine air bubbles on the surfaces of polycaprolactone (PCL), polyamide 66 (PA66), and polyvinylchloride (PVC) particles during the settling velocity experiments.

depends on τ_{epi}/τ_{hypo}, which can be expressed as $\frac{\nu_{s\_epi}}{\nu_{s\_hypo}} \cdot \frac{z_{epi}}{z_{hypo}}$. The relationship $N_{epi}/N_{hypo} = f(\nu_{s\_epi}/\nu_{s\_hypo}, z_{epi}/z_{hypo})$ is universally valid for all types of microplastics (independent of size, shape, and density) as long as the ratio ν_{s_epi}/ν_{s_hypo} in a lake system is constant. This implies that N_{epi}/N_{hypo} only depends on lake characteristics such as the temperature and thickness of each compartment.

Results

Settling velocities of pristine particles

The settling velocities for the six polymers ranged between ~ 0.30 and ~ 50 mm s^{-1} (Fig. 2). Supporting Information Fig. S6 presents the distribution of the CSF of the microplastic particles. The results show a clear dependence of the settling velocities on particle size, with a coefficient of determination (R^2) between 0.70 and 0.81 and a high statistical significance ($p < 0.001$). In addition, the effect of polymer density on the settling velocity was clearly visible in the slope of the regression lines. Polymers with high density were consistently associated with a steeper slope, and thus a faster settling velocity. The calculated Reynolds number for the particles varied between 0.05 and 130, thus being at the transition between laminar and the intermediate regimes.

Biofilm-coated particles

No significant changes were observed in the density, shape, or roundness of the incubated particles, even after 30 weeks of incubation (Supporting Information Fig. S7). However, the confocal laser scanning microscope images at 10 weeks incubation clearly showed a varying abundance of biofilms on the microplastic particle surface (Fig. 3). These were mainly composed of microbial cells and extra polymeric substances. The surfaces of the particles were only partially covered with biofilm, where it was concentrated in a few dense spots.

The potential formation of aggregates was investigated by incubating various polystyrene particles with an average equivalent diameter between 300 and 350 μm for 10 weeks in a single tube. The sample shown in Fig. 4 has a high abundance of extra polymeric substances despite the surface of the particles not being densely colonized by microbial cells. It also shows that individual polystyrene particles in combination

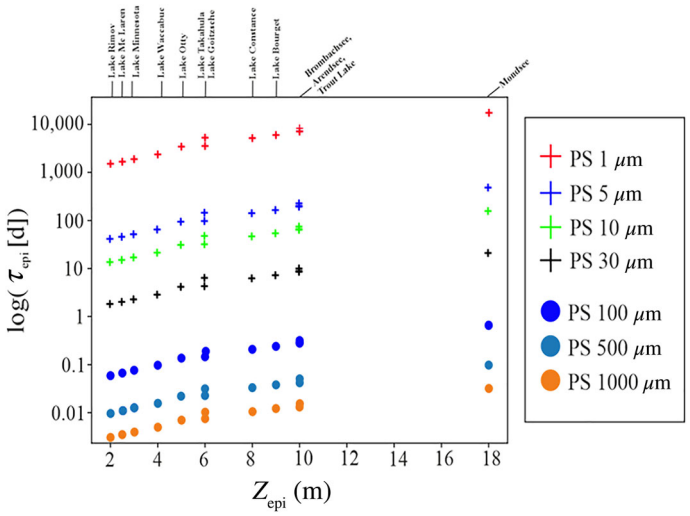

Fig. 7. Dependency of the mean residence time τ (d) on the particle size of the polystyrene (PS) particles, and depth of the epilimnion Z_{epi} (m). Note the logarithmic scale.

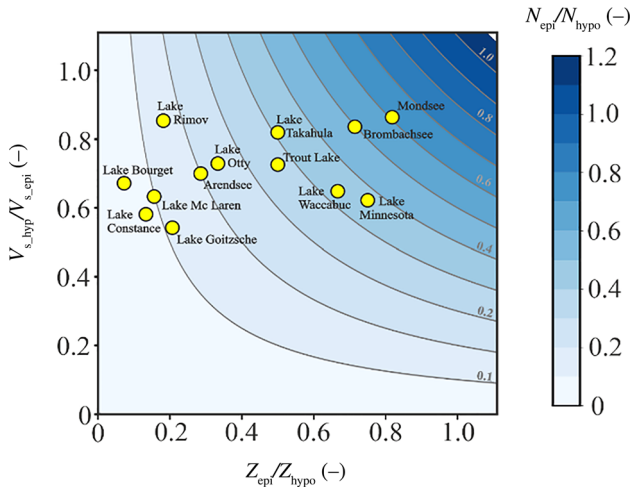

Fig. 8. Relative abundance for microplastics (N_{epi}/N_{hypo}) in the epilimnion and hypolimnion assuming steady-state conditions for different lake systems as a function of the settling velocity (v_{s_hypo}/v_{s_epi}) and depth (z_{epi}/z_{hypo}) ratios.

with the extra polymeric substances form a larger aggregate with the biofilm appearing to act as an "adhesive."

After 6, 8, 10, and 30 weeks of incubation, no substantial differences in sedimentation rates between pristine and incubated microplastic particles were observed (Supporting Information Fig. S8). The maximum deviation in the mean settling velocities was ± 5% which is within the measurement error of the particle image velocimetry system. An *F*-test and paired *t*-test confirmed that there was no significant difference ($p > 0.05$) before and after incubation in either means or variance. Both incubated and pristine particles followed much the same settling trajectories after the incubation periods (Supporting Information Fig. S9).

Calculated settling velocity

Despite significant scatter in the data, the measured settling velocities were systematically lower than those calculated using Dietrich (1982) (Fig. 5). The nonbiodegradable particles had significantly less scatter around the 1 : 1 line than biodegradable polymers (Fig. 5). During the experiments, it was observed that fine air bubbles tend to attach to the surfaces of all polymer types and most obviously on the biodegradable microplastic particles (Fig. 6), despite all particles being pretreated in an ultrasonic bath prior to the experiments.

Residence times of microplastics in stratified lakes

The effect of particle size on the mean residence time in the epilimnion for 13 different lake systems is shown in Fig. 7. The mean depths of the epilimnion (z_{epi}) during summer during stratified conditions ranged from 2 to 18 m. The modeled epilimnic mean residence times for the various lakes depended strongly on particle size and to a lesser extent on the polymer type. For the large microplastic particles (100–1000 μm), the modeled mean residence time was less than 1 d for all lakes. In contrast, the mean residence times for the smallest microplastic particles (1–30 μm) were orders of magnitudes higher, with residence times up to 10,000 d for 1-μm particles in the Mondsee.

Relative particle abundance (N_{epi}/N_{hypo}) for the selected lake systems during steady-state conditions is shown in Fig. 8. These lakes show a large variation in the z_{epi}/z_{hypo} ratios, ranging between 0.1 and 0.8. As the lake data was measured entirely during stratification in the summer months, water temperatures for the hypolimnion were consistently lower than the epilimnion, leading to $v_{s\_hypo}/v_{s\_epi} < 1$ (higher viscosities in the cold hypolimnion). The N_{epi}/N_{hypo} ranged between < 0.1 for the larger lakes such as Lake Constance in Germany and 0.6 for the Mondsee in Austria and shows that the proportion of microplastics found in either the epilimnion or hypolimnion scales with the z_{epi}/z_{hypo}. Interestingly, the Mondsee has the highest N_{epi}/N_{hypo} ratio (> 0.6), meaning the majority of microplastics will be found in the epilimnion and the highest mean epilimnic residence time (~ 10,000 d for 1-μm particles). This maximizes the probability of microplastic uptake by filter feeders and other organisms at the base of the food chain that are generally found in the epilimnion. In contrast, for Lake Constance, Lake Bourget, and Lake McLaren most of the microplastics should be found in the hypolimnion ($N_{epi}/N_{hypo} < 0.1$) despite often substantial residence time in the epilimnion (Fig. 8).

As an example to demonstrate how the redistribution of particles occurs between the different lake compartments, the dynamic model was used to calculate the flux of polystyrene spheres (Supporting Information Fig. S10) with a size range of 1, 10, 500, and 1000 μm to a virtual lake loosely based on Upper Lake Constance (Fig. 9). One hundred meters of the stratified lake water column were modeled using the data from

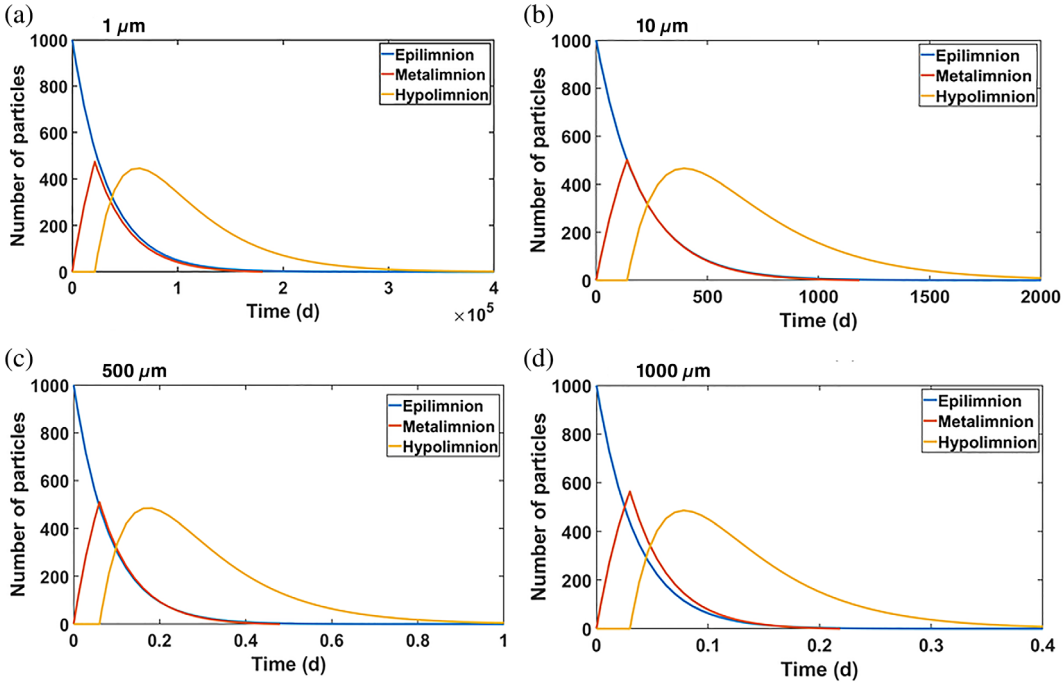

Fig. 9. Simulation results of 1-, 10-, 500-, and 1000-μm polystyrene spheres showing the modeled numbers of the accumulated microplastics in each lake compartment vs. elapsed time in Upper Lake Constance on Day 319 according to lake data from Appt et al. (2004). The simulations were initiated with a pulse of 1000 spherical polystyrene particles uniformly distributed in the well-mixed epilimnion.

Appt et al. (2004) (Supporting Information Table S11). The simulations were initiated with a pulse of 1000 spherical polystyrene particles that were uniformly distributed in the well-mixed epilimnion (Fig. 9). The microplastic numbers in the epilimnion decreased exponentially following the pulse. In contrast, in the metalimnion and the hypolimnion, the microplastic particles initially increased as they received particles from the overlying lake layer. Microplastic numbers in the metalimnion and hypolimnion started to decrease after the loss rate to the underlying layer (or sediment in the case of the hypolimnion) exceeded the input rate from the overlying layer. The modeling results showed that the residence time τ (d) in each layer was very strongly dependent on particle size, similarly to the steady-state model.

Discussions

Various factors such as particle size, polymer density, hydrophobicity of the particle surface, biofouling, water temperature, and turbulent mixing control the residence times of microplastics in lakes. These factors, combined with high or constant input of microplastics will increase the probability that microplastics will be ingested by aquatic organisms and potentially be transferred within the lake food chain (Nelms et al. 2018).

The experimentally determined settling velocities showed that the density and size of the microplastics are the most critical parameters controlling the settling velocity. Since the microplastic settling velocity during laminar conditions depends on their weight, drag forces, and buoyancy forces, all large and dense particles have significantly higher settling velocities than the smaller and lighter microplastics.

As the CSF describes the flatness of the particle and it depends only on the ratio between the three axes of the particles rather than its size, it was experimentally difficult to isolate the effect of particle shape on the settling velocity, separating it from that of density and size. This problem was exacerbated by the fact that all particles were similar in shape, despite being irregular (having similar CSF) (Supporting Information Fig. S1, S2) and no fibers or special geometric objects such as cubes, cylinders, or discs were used in the experiments.

We originally expected rapid and somewhat uniform colonization of the particles by biofilms (Zettler et al. 2013; Rummel et al. 2017). However, the confocal laser scanning microscope images showed that the biofilm rather forms dense patches with large parts of the particles left uncolonized. The formation of biofilm and in particular the presence of a thick extra polymeric substance increased the tendency for microplastic aggregation, which is consistent with findings from Rummel et al. (2017). Such aggregates are larger and likely to have different surface properties, densities, and shapes compared to the pristine particles, which should result in different physical behavior within the water column (Leiser et al. 2020).

The literature suggests that the colonization process alters the polarity of the plastic surface, changing it from hydrophobic to hydrophilic (Michels et al. 2018; Tu et al. 2020; van

Melkebeke et al. 2020), increases the density of the particle (Rummel et al. 2017; Michels et al. 2018), and reduces the attachment of air bubbles on the surface (Renner et al. 2020). Therefore, it was anticipated that the settling velocity would increase after incubation. However, no measurable changes in the physical properties or sedimentation behavior were observed. This may be due to the "short" incubation periods of 6, 8, 10, and 30 weeks. Also, the pond was frozen for the first 3 weeks of incubation during the winter season which may explain the small volumes of biofilm accumulated on the particle surface, assuming that the metabolism of the biofilm-building organisms was affected by the low temperatures (Farhat et al. 2016).

In accordance with Waldschläger and Schüttrumpf (2019); van Melkebeke et al. (2020), the settling velocities of the microplastics were not well described using the traditional sediment settling equation of Dietrich (1982). We believe this is due to the hydrophobicity of the microplastic surfaces, which is conducive to the formation of fine air bubbles, which then increased the buoyancy force exerted on the settling particle and reduced their settling velocity. Since Dietrich (1982) was originally developed for mineral particles, the hydrophobic adhesion between microplastics and air bubbles did not play a role in the settling behavior. Whether microplastic remains hydrophobic in the environment or not likely depends on microplastic surface properties, for example, after biofilm colonization. Pristine microplastics are unlikely to be found in natural aquatic environments as they are usually rapidly colonized by biofilms or adsorb natural material such as dissolved organic carbon or mineral precipitates (e.g., iron oxides) (Leiser et al. 2020). Also, measuring the size of particles from two-dimension images may not properly capture the third dimension of the particles. This is a potential source of error in the calculations of the theoretical settling velocities. These observations suggest, however, that the settling behavior of microplastic is more complex than in simplified theoretical models and more advanced methods such as computational fluid dynamics should be used to investigate this more exactly.

In the lake model, the epilimnion and the hypolimnion were presented as well-mixed systems to mimic turbulent processes within these layers during the thermal stratification. In contrast, the metalimnion was assumed to be laminar. The residence time of microplastics in the metalimnion is relatively short compared to the epilimnion and hypolimnion due to the lack of mixing processes as well as to a limited thickness. The extremely long residence time for small microplastic particles in the epilimnion in particular forms a high uptake probability for aquatic organisms such as filter feeders. This lake model has, however, a highly simplified and theoretical representation of residence times in the three lake compartments. Real lake systems are considerably more complex than these simplified representations of lake physics. In real lakes, the residence times of the settling microplastics are likely coupled with the changes in lakes' hydrodynamics such as temperature fluctuation, waves, transient turbulence, or lake mixing in autumn and spring as stratification destabilizes. Also, lake retention time (flushing time), which is strongly dependent on the internal physical processes and water fluxes from the catchment (Ambrosetti et al. 2003), plays a decisive role in how long the microplastics will actually reside in a lake, and thus how long organisms have the opportunity to ingest them. Calculated residence times were on the order of 10^5 d for the smallest particles, meaning that the flushing time is significantly shorter than the residence time for most lakes, and thus is not really a meaningful number for a real lake system such as Lake Constance, which has a theoretical average flushing time of 4.5 years (Wessels 2015). It does suggest, however, that there should only be a negligible amount of microplastics of this size range found in the lake sediments unless some process increases their settling velocity, for example, aggregation with existing lake particles and detritus or uptake and death of organisms or egestion via fecal pellets. In addition, the biologically driven mixing of the water column due to the vertical migration of zooplankton increase turbulence in the water column (Dean et al. 2016) which may cause resuspension and redistribution of the microplastics, which may be particularly important in the hypolimnion.

Conclusion

This research aimed to identify the primary controls and time scales of microplastic residence times in stratified lake systems. By combining laboratory experiments and modeling, it was clear that microplastic residence times in the lake water column highly depend on the size and to a less extent the density of the particle, varying over many orders of magnitude. The comparison between laboratory-measured and calculated settling velocities using Dietrich (1982) showed that hydrophobic surface properties of the pristine microplastics are a key factor that needs to be considered when estimating settling velocities. It is expected that the hydrophobic adhesion between pristine microplastics and fine air bubbles can increase the buoyancy forces exerted on the particles and increase their residence time in the lake water column.

The microplastic polymers incubated in a small lake were effectively and rapidly colonized by biofilm and included bacteria cells and extra polymeric substances. However, the settling experiments did not show any substantial differences in the sedimentation trajectories and velocities between individual (i.e., not aggregates) pristine and incubated microplastics. The presence of biofilms on the surfaces of incubated microplastics did tend to favor the formation of aggregates. These aggregates are expected to sink faster and to have shorter residence time than individual pristine microplastics because of their increase in size and changes in surface properties.

Our lumped parameter modeling approach is a simple way to estimate residence times, fluxes, and numbers of microplastics in the epilimnion, metalimnion, and hypolimnion during both steady-state and dynamic conditions. The functional relationship

N_{epi}/N_{hypo} allows a rapid assessment of where most microplastics will be found in different lakes and is independent of the input influx to the lake as long as the ratio v_{s_epi}/v_{s_hypo} is constant. Also, the modeling approach was capable of showing the dynamic redistribution of microplastics in the stratified lake water column. The accumulated numbers and residence times of microplastics in the three lake compartments varied over several orders of magnitude and were strongly dependent on particle size as well as physical lake properties such as depth and temperature of the hypolimnion, metalimnion, and epilimnion. This is crucial for the uptake of microplastics by, for example, filter feeders, in lake systems. The simulated residence times suggest that significant numbers of microplastics should be found in lake sediment as long as their residence time is shorter than lake flushing time. In contrast, small microplastics with residence times significantly longer than lake flushing time are unlikely to be found in large numbers in lake sediment unless some biological or physical processes increase their settling velocity to deliver them to the lake bottom.

Data availability statement

Data are archived on CRC 1357 cloud storage and available on request.

References

Agarwal, S. 2020. Biodegradable polymers: Present opportunities and challenges in providing a microplastic-free environment. Macromol. Chem. Phys. **221**: 2000017. doi:10.1002/macp.202000017

Aljaibachi, R., and A. Callaghan. 2018. Impact of polystyrene microplastics on Daphnia magna mortality and reproduction in relation to food availability. PeerJ **6**: e4601. doi:10.7717/peerj.4601

Ambrosetti, W., L. Barbanti, and N. Sala. 2003. Residence time and physical processes in lakes. J. Limnol. **62**: 1. doi:10.4081/jlimnol.2003.s1.1

Appt, J., J. Imberger, and H. Kobus. 2004. Basin-scale motion in stratified Upper Lake Constance. Limnol. Oceanogr. **49**: 919–933. doi:10.4319/lo.2004.49.4.0919

Arthur, C., J. Baker, and H. Bamford. 2009. Proceedings of the International Research Workshop on the Occurrence, Effects and Fate of Microplastic Marine Debris, 9–11 September 2008. NOAA Technical Memorandum NOS-OR&R-30.

Bagaev, A., A. Mizyuk, L. Khatmullina, I. Isachenko, and I. Chubarenko. 2017. Anthropogenic fibres in the Baltic Sea water column: Field data, laboratory and numerical testing of their motion. Sci. Total Environ. **599–600**: 560–571. doi:10.1016/j.scitotenv.2017.04.185

Bellasi, A., G. Binda, A. Pozzi, S. Galafassi, P. Volta, and R. Bettinetti. 2020. Microplastic contamination in freshwater environments: A review, focusing on interactions with sediments and benthic organisms. Environments **7**: 30. doi:10.3390/environments7040030

Browne, M. A., T. Galloway, and R. Thompson. 2007. Microplastic—An emerging contaminant of potential concern? Integr. Environ. Assess. Manag. **3**: 559–561. doi:10.1002/ieam.5630030412

Cole, M., P. K. Lindeque, E. Fileman, J. Clark, C. Lewis, C. Halsband, and T. S. Galloway. 2016. Microplastics alter the properties and sinking rates of zooplankton faecal pellets. Environ. Sci. Technol. **50**: 3239–3246. doi:10.1021/acs.est.5b05905

Dean, C., A. Soloviev, A. Hirons, T. Frank, and J. Wood. 2016. Biomixing due to diel vertical migrations of zooplankton: Comparison of computational fluid dynamics model with observations. Ocean Model. **98**: 51–64. doi:10.1016/j.ocemod.2015.12.002

Dietrich, W. E. 1982. Settling velocity of natural particles. Water Resour. Res. **18**: 1615–1626. doi:10.1029/WR018i006p01615

Farhat, N. M., J. S. Vrouwenvelder, M. C. M. van Loosdrecht, S. S. Bucs, and M. Staal. 2016. Effect of water temperature on biofouling development in reverse osmosis membrane systems. Water Res. **103**: 149–159. doi:10.1016/j.watres.2016.07.015

Fischer, E. K., L. Paglialonga, E. Czech, and M. Tamminga. 2016. Microplastic pollution in lakes and lake shoreline sediments—a case study on Lake Bolsena and Lake Chiusi (Central Italy). Environ. Pollut. **213**: 648–657. doi:10.1016/j.envpol.2016.03.012

Geyer, R., J. R. Jambeck, and K. L. Law. 2017. Production, use, and fate of all plastics ever made. Sci. Adv. **3**: e1700782. doi:10.1126/sciadv.1700782

Ghawi, A. H., and J. Kris. 2012. A computational fluid dynamics model of flow and settling in sedimentation tanks. *In* H. W. Oh [ed.], Computational fluid dynamics (CFD) and discrete element method (DEM) applied to centrifuges. INTECH Open Access Publisher.

Kaiser, D., N. Kowalski, and J. J. Waniek. 2017. Effects of biofouling on the sinking behavior of microplastics. Environ. Res. Lett. **12**: 124003. doi:10.1088/1748-9326/aa8e8b

Khatmullina, L., and I. Isachenko. 2017. Settling velocity of microplastic particles of regular shapes. Mar. Pollut. Bull. **114**: 871–880. doi:10.1016/j.marpolbul.2016.11.024

Kirillin, G., H.-P. Grossart, and K. W. Tang. 2012. Modeling sinking rate of zooplankton carcasses: Effects of stratification and mixing. Limnol. Oceanogr. **57**: 881–894. doi:10.4319/lo.2012.57.3.0881

Lacerda, A. L. D. F., and others. 2019. Plastics in sea surface waters around the Antarctic Peninsula. Sci. Rep. **9**: 3977. doi:10.1038/s41598-019-40311-4

Lampert, W., and U. Sommer. 2010. Limnoecology. *In* The ecology of lakes and streams, 2nd ed. Univ. Press.

Leiser, R., G.-M. Wu, T. R. Neu, and K. Wendt-Potthoff. 2020. Biofouling, metal sorption and aggregation are related to sinking of microplastics in a stratified reservoir. Water Res. **176**: 115748. doi:10.1016/j.watres.2020.115748

Meides, N., and others. 2021. Reconstructing the environmental degradation of polystyrene by accelerated weathering. Environ. Sci. Technol. **55**: 7930–7938. doi:10.1021/acs.est.0c07718

Michels, J., A. Stippkugel, M. Lenz, K. Wirtz, and A. Engel. 2018. Rapid aggregation of biofilm-covered microplastics with marine biogenic particles. Proceedings. Biological sciences **285**: 20181203. doi:10.1098/rspb.2018.1203

Nelms, S. E., T. S. Galloway, B. J. Godley, D. S. Jarvis, and P. K. Lindeque. 2018. Investigating microplastic trophic transfer in marine top predators. Environ. Pollut. **238**: 999–1007. doi:10.1016/j.envpol.2018.02.016

Nguyen, T. H., F. H. M. Tang, and F. Maggi. 2020. Sinking of microbial-associated microplastics in natural waters. PLoS One **15**: e0228209. doi:10.1371/journal.pone.0228209

Nishri, A., A. Rimmer, and Y. Lechinsky. 2015. The mechanism of hypolimnion warming induced by internal waves. Limnol. Oceanogr. **60**: 1462–1476. doi:10.1002/lno.10109

Ramsperger, A. F. R. M., and others. 2020. Structural diversity in early-stage biofilm formation on microplastics depends on environmental medium and polymer properties. Water **12**: 3216. doi:10.3390/w12113216

Renner, G., A. Nellessen, A. Schwiers, M. Wenzel, T. C. Schmidt, and J. Schram. 2020. Hydrophobicity-water/air-based enrichment cell for microplastics analysis within environmental samples: A proof of concept. MethodsX **7**: 100732. doi:10.1016/j.mex.2019.11.006

Reynolds, C. S. 1984. The ecology of freshwater phytoplankton. Cambridge Univ. Press.

Reynolds, C. S. 2006. The ecology of phytoplankton. Cambridge Univ. Press.

Reynolds, C. S., and S. W. Wiseman. 1982. Sinking losses of phytoplankton in closed limnetic systems. J. Plankton Res. **4**: 489–522. doi:10.1093/plankt/4.3.489

Rocha-Santos, T., and A. C. Duarte. 2015. A critical overview of the analytical approaches to the occurrence, the fate and the behavior of microplastics in the environment. TrAC Trends Anal. Chem. **65**: 47–53. doi:10.1016/j.trac.2014.10.011

Rummel, C. D., A. Jahnke, E. Gorokhova, D. Kühnel, and M. Schmitt-Jansen. 2017. Impacts of biofilm formation on the fate and potential effects of microplastic in the aquatic environment. Environ. Sci. Technol. Lett. **4**: 258–267. doi:10.1021/acs.estlett.7b00164

Schindelin, J., and others. 2012. Fiji: An open-source platform for biological-image analysis. Nat. Methods **9**: 676–682. doi:10.1038/nmeth.2019

Singh, P., J. Bagrania, and A. K. Haritash. 2019. Seasonal behaviour of thermal stratification and trophic status in a sub-tropical Palustrine water body. Appl. Water Sci. **9**: 139. doi:10.1007/s13201-019-1011-z

Sun, J., X. Dai, Q. Wang, M. C. M. van Loosdrecht, and B.-J. Ni. 2019. Microplastics in wastewater treatment plants: Detection, occurrence and removal. Water Res. **152**: 21–37. doi:10.1016/j.watres.2018.12.050

Toussaint, B., and others. 2019. Review of micro- and nanoplastic contamination in the food chain. Food Addit. Contam. Part A Chem. Anal. Control Expo. Risk Assess. **36**: 639–673. doi:10.1080/19440049.2019.1583381

Tu, C., T. Chen, Q. Zhou, Y. Liu, J. Wei, J. J. Waniek, and Y. Luo. 2020. Biofilm formation and its influences on the properties of microplastics as affected by exposure time and depth in the seawater. Sci. Total Environ. **734**: 139237. doi:10.1016/j.scitotenv.2020.139237

van Melkebeke, M., C. Janssen, and S. de Meester. 2020. Characteristics and sinking behavior of typical microplastics including the potential effect of biofouling: Implications for remediation. Environ. Sci. Technol. **54**: 8668–8680. doi:10.1021/acs.est.9b07378

Waldschläger, K., and H. Schüttrumpf. 2019. Effects of particle properties on the settling and rise velocities of microplastics in freshwater under laboratory conditions. Environ. Sci. Technol. **53**: 1958–1966. doi:10.1021/acs.est.8b06794

Wessels, M. 2015. Bathymetry of Lake Constance—A high-resolution survey in a large, deep Lake. zfv – Zeitschrift für Geodäsie, Geoinformation und Landmanagement. **140**: 203–210. doi:10.12902/zfv-0079-2015

Worm, B., H. K. Lotze, I. Jubinville, C. Wilcox, and J. Jambeck. 2017. Plastic as a persistent marine pollutant. Annu. Rev. Env. Resour. **42**: 1–26. doi:10.1146/annurev-environ-102016-060700

Wright, S. L., R. C. Thompson, and T. S. Galloway. 2013. The physical impacts of microplastics on marine organisms: A review. Environ. Pollut. **178**: 483–492. doi:10.1016/j.envpol.2013.02.031

Zettler, E. R., T. J. Mincer, and L. A. Amaral-Zettler. 2013. Life in the "plastisphere": Microbial communities on plastic marine debris. Environ. Sci. Technol. **47**: 7137–7146. doi:10.1021/es401288x

Acknowledgments

Funded by the Deutsche Forschungsgemeinschaft (DFG, German Research Foundation)—Project Number 391977956—SFB 1357. The authors would like to thank Peter Strohriegl for providing microplastic particles for the settling experiments, Antonia Freiberger for her support during confocal laser scanning microscope experiments, and Ulrich Mansfeld and Martina Heider for the scanning electron microscope images. Open Access funding enabled and organized by Projekt DEAL.

Conflict of interest

None declared.

Submitted 09 August 2021
Revised 16 November 2021
Accepted 06 February 2022

Associate editor: Yong Liu